Kinetics and Catalysis, Vol. 43, No. 5, 2002, pp. 698–710. Translated from Kinetika i Kataliz, Vol. 43, No. 5, 2002, pp. 747–760.

Catalytic and Physicochemical Properties of Oxidative Condensation Products in the Oxidative Dehydrogenation of Propane by Sulfur Dioxide on SiO_2

I. G. Danilova, E. A. Paukshtis, A. V. Kalinkin, A. L. Chuvilin, G. S. Litvak, A. A. Altynnikov, and V. F. Anufrienko

Boreskov Institute of Catalysis, Siberian Division, Russian Academy of Sciences, Novosibirsk, 630090 Russia

Received December 21, 2001

Abstract—The effect of the deposition of oxidative condensation products in the reaction of oxidative propane dehydrogenation in the presence of SO_2 on the catalytic, acid–base, and texture characteristics of silica was studied. It was found that the oxidative condensation products exhibited high catalytic activity in this reaction. The carbonization of silica from 0 to ~40 wt % was accompanied by an increase in the yield of propylene from 3.4 to 46 mol % (640°C; a $C_3H_8/SO_2/He + N_2$ mixture, 10 : 10 : 80 vol %). Further accumulation of condensation products resulted in a considerable decrease in the pore volume and radius; this imposed diffusion limitations on both propane conversion and selectivity to propane conversion products. The nature of active and deactivated condensation products was studied by DRIFT spectroscopy, diffuse-reflectance UV–VIS spectroscopy, EPR spectroscopy, XPS, thermal analysis, and electron microscopy.

INTRODUCTION

Early publications [1–3] on the activity of carbon materials in the oxidative dehydrogenation of hydrocarbons were concerned with the catalytic abilities of organic polymers. Their role in catalysis was related to the occurrence of paramagnetic centers and functional groups containing O and N atoms. Oxidative condensation products (OCP), which are formed and accumulated in the course of reaction on acid catalysts, were identified as an active component in the oxidative dehydrogenation reactions of alkylbenzenes (in the presence of O_2 or SO_2) [4–9] or in the ammoxidation reaction of toluene [8]. It was found that polycyclic compounds containing O, S, or N atoms with a developed system of conjugated bonds and a high concentration of paramagnetic centers are catalytically active OCP [4, 7–9]. The activity and selectivity of propylene formation in the oxidative dehydrogenation of propane by sulfur dioxide was found to increase in the course of accumulation of OCP containing C, H, O, and S atoms on the surface of alumina, silica, and gallium oxide. Fe, Bi, and Pb oxides underwent sulfidation in the course of reaction to result in a decrease in the yield of propylene [10, 11].

In this work, we report on a study of the formation and deactivation of active OCP in the course of the oxidative dehydrogenation of propane by sulfur dioxide on SiO_2. The effect of carbon deposits on the catalytic, acid–base, and texture characteristics of silica was studied. The nature of active and deactivated OCP was examined by DRIFT spectroscopy, diffuse-reflectance UV–VIS spectroscopy, EPR spectroscopy, XPS, thermal analysis, and electron microscopy.

EXPERIMENTAL

Catalytic experiments were performed in a flow setup at 640°C, a contact time ((τ) of 10 s, and atmospheric pressure. silica of KSKG grade (S_{sp} = 40 m^2/g; impurity concentrations according to chemical analysis data: Al, 0.07 wt % and Na, 0.18 wt %) with a particle size of 0.25–0.5 mm and a volume of 1 cm^3 was placed in a U-shaped quartz reactor and heated to a reaction temperature in a helium flow before the addition of a reaction mixture. To decrease the contribution of a homogeneous reaction, the free volume of the reactor was packed with quartz chips with a particle size of 0.25–0.5 mm [12]. In the absence of a catalyst from the reactor packed with quartz chips, the conversion of propane was no higher than 2.2% [13]. The reaction mixtures (dilute mixture **I** of C_3H_8, SO_2, He, and N_2, 10 : 10 : 79 : 1 vol % and concentrated mixture **II** of C_3H_8, SO_2, and N_2, 79.5 : 19.5 : 1 vol %) and reaction products were analyzed by chromatography.

The thermal analysis of carbonized samples was performed on a DQ 1500-D derivatograph in a temperature range of 20–1000°C at a heating rate of 10 K/min in air; the sample weight was 0.1 g.

The texture characteristics of the samples were calculated from low-temperature (77 K) nitrogen adsorption isotherms measured on an ASAP 2400 instrument from Micrometrics (USA). The average pore diameter (D) was calculated from BET data using the cylinder equation ($D = 4V/S_{BET}$) [14]. The pore volume distribu-

0023-1584/02/4305-0698$27.00

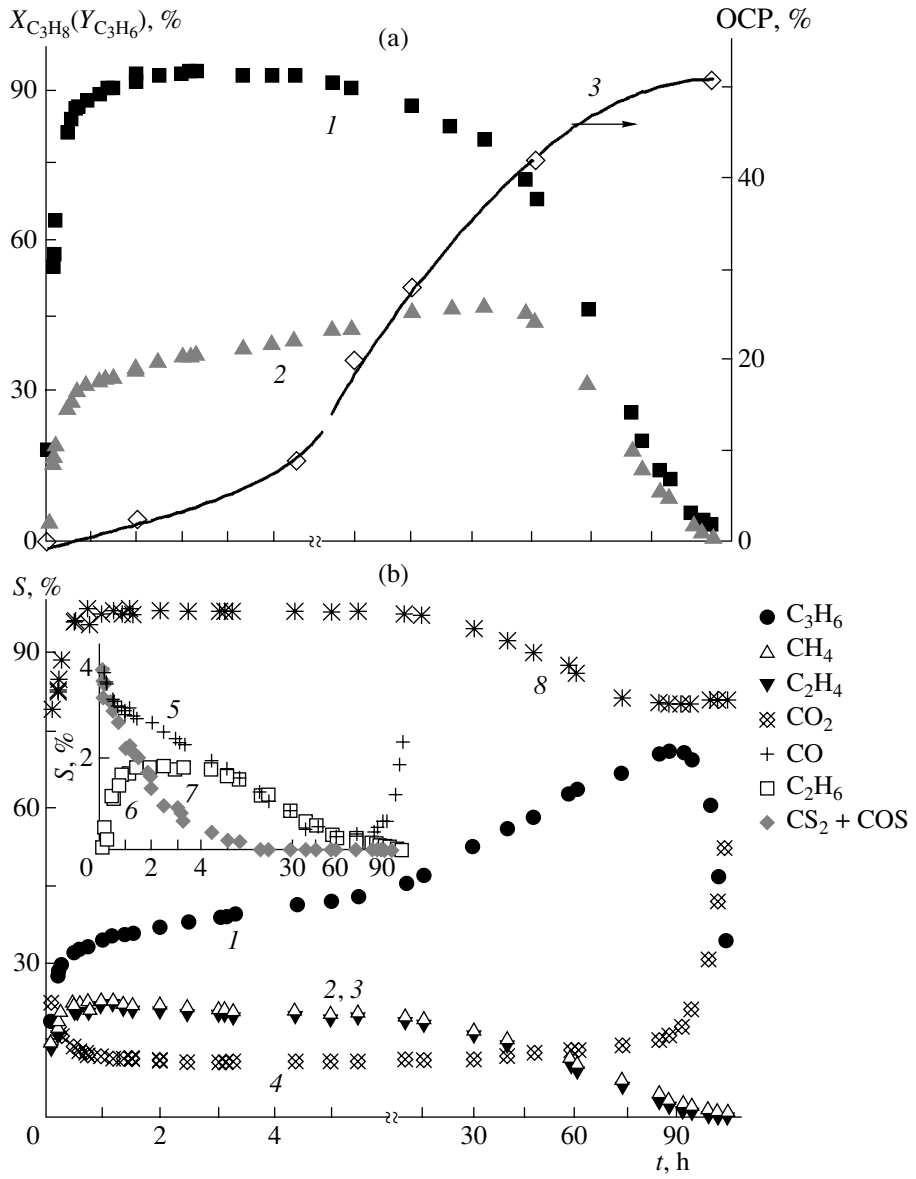

Fig. 1. Catalytic properties of SiO_2 as functions of reaction time in the oxidative dehydrogenation of propane (mixture **I** 640°C, τ = 10 s). (a) (*1*) Propane conversion $X_{C_3H_8}$, (*2*) propylene yield $Y_{C_3H_6}$, and (*3*) OCP deposition in the course of reaction. (b) Selectivity to the propane conversion products: (*1*) C_3H_6, (*2*) CH_4, (*3*) C_2H_4, (*4*) CO_2, (*5*) CO, (*6*) C_2H_6, and (*7*) CS_2 + COS. (*8*) Balance on carbon, as calculated taking into account gaseous products.

tion was calculated from the desorption branches of the hysteresis loops of adsorption isotherms in terms of a model of disjoint cylindrical pores. Before the experiments, all samples were subjected to thermal vacuum treatment at 300°C for 20 h for the removal of adsorbed water.

The XPS spectra were measured on a VG ESCA-3 spectrometer using AlK_α radiation; $h\nu$ = 1486.6 eV. The test samples of catalysts were fixed in a holder with the use of a double-sided adhesive tape. The binding energies of the elements were calculated with the use of the Si2*p* line as an internal standard, whose value was taken as equal to 103.5 eV (for SiO_2 [15]). The surface concentrations of the elements were calculated based on empirical sensitivity factors for the elements, which were given by Briggs and Seah [16] for analyzers with constant transmission energy.

The concentrations of acid–base centers on the surfaces of coked silicas were determined by direct titration with the solutions of weak acids or bases with different pK_a values according to the published procedure [17]. The UV spectra were measured on a Specord UV–VIS spectrophotometer.

The DRIFT spectra were measured on a Bruker IFS-113v FTIR spectrometer over a range of 1000–

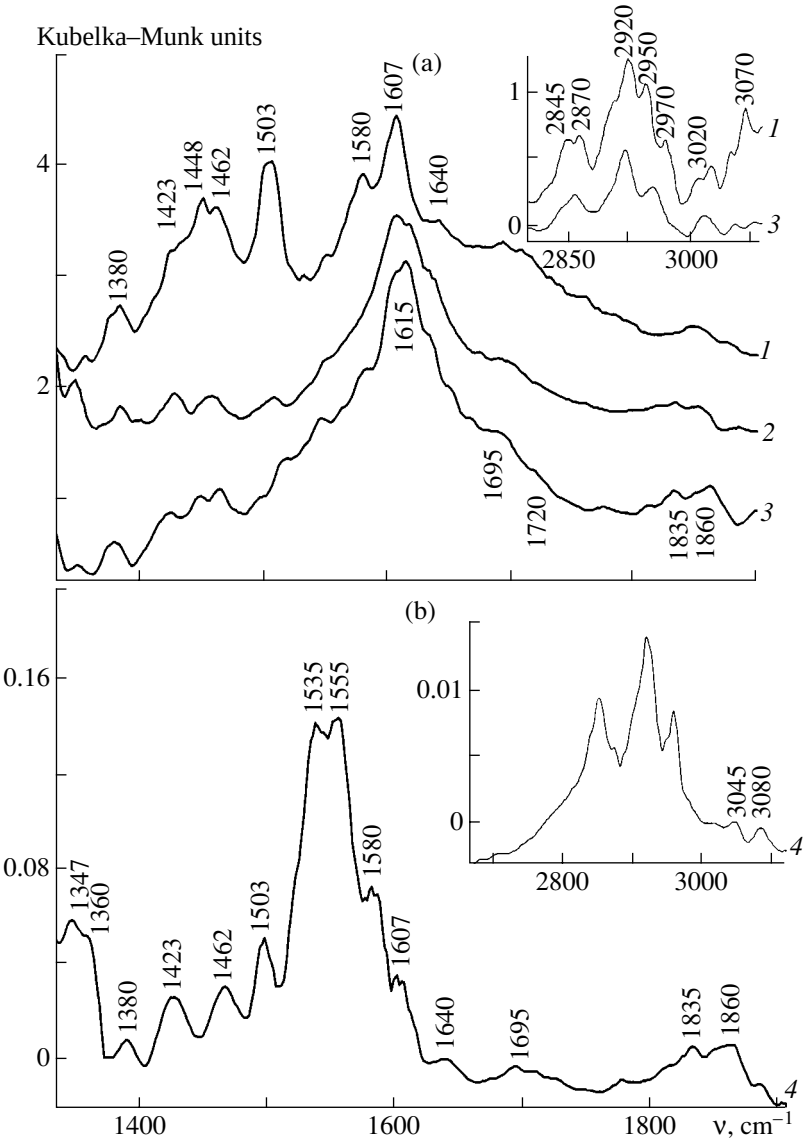

Fig. 2. DRIFT spectra of OCP deposited on SiO_2 for (*1*) 0.5, (*2*) 2, (*3*) 6, and (*4*) 12 h. Spectra *1–3* were obtained by the difference between the spectra of a sample and the initial SiO_2.

6000 cm^{-1} with a resolution of 4 cm^{-1} using a homemade diffuse-reflectance attachment. The spectra were treated by converting the experimental absorption band intensities into the Kubelka–Munk values $F(R)$ [18]: $F(R) = (1 - R)^2/2R$, where R is the experimentally measured IR reflectance of the sample layer. The diffuse-reflectance UV–VIS spectra were measured on a Shimadzu UV-300 spectrometer with the use of a standard diffuse-reflectance attachment.

The EPR spectra were measured on a JES-3BX instrument at 77 and 300 K. The samples were preevacuated to a residual pressure of 10^{-2} torr at 300°C.

The micrographs of the samples were taken on a JEM 2010 transmission electron microscope.

RESULTS AND DISCUSSION

The initial SiO_2 exhibited a low catalytic activity in the oxidative dehydrogenation of propane in the presence of sulfur dioxide: 5 min after the addition of a reaction mixture, the conversion of propane was $X_{C_3H_8}$ = 18% and the selectivity to propylene was $S_{C_3H_6}$ = 19% (Fig. 1). The conversion of C_3H_8 increased from 18 to 93% in the first hour of catalyst operation, and it remained unchanged for ~20 h. In the next ~40 h, the conversion of propane gradually decreased to 70% and then decreased to 3% after 105 h of operation (Fig. 1a). The yield of propylene increased from 3.4 to 32% in the first hour of catalyst operation and to 40% in the next ~5 h; then, it slowly increased up to 46% for ~50 h. The further operation of the catalyst resulted in a decrease

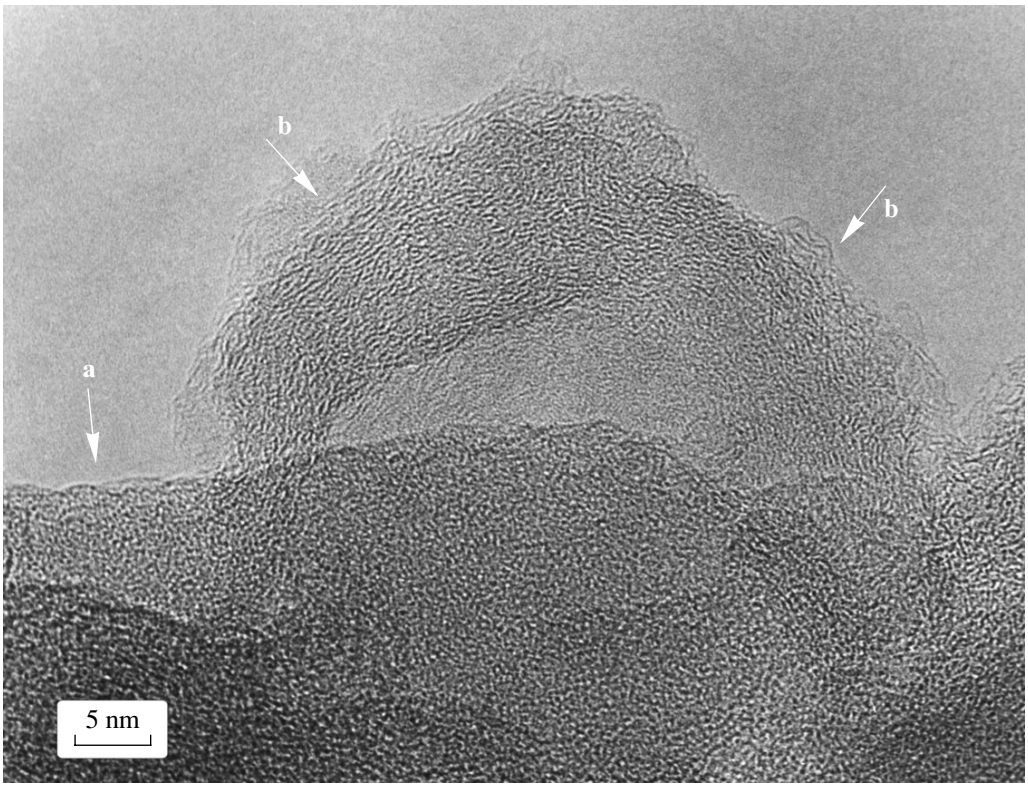

Fig. 3. Micrograph of sample OCP (6 h)/SiO_2. Arrows indicate (a) the pure surface of an SiO_2 pellet and (b) OCP.

in the conversion and the yield of propylene. In the course of reaction, OCP were formed and gradually accumulated on silica (Fig. 1a). Evidently, the genesis of OCP is responsible for the change in catalytic properties. The following three periods in the operation of the catalyst for propane conversion into propylene can be distinguished: activation, ~2–6 h; a quasi-steady state (a period of insignificant changes in the catalytic properties), ~50–55 h; and deactivation. Let us consider changes in the properties of the catalyst in different periods of operation.

A Study of the Formation of an Active Component

A dramatic increase in the conversion of C_3H_8 and a simultaneous increase in selectivity to propylene from 19 to 32% were observed within the first 30 min of the reaction of oxidative propane dehydrogenation on SiO_2

Table 1. Changes in the acid and base properties of SiO_2 on the deposition of OCP in the course of the oxidative dehydrogenation of propane

Entry	Sample	Concentration of acid sites, μmol/m^2		Concentration of basic sites, μmol/m^2	
		total (pK_a = 11.1)*	strong acid sites (pK_a = 0.8)**	total (pK_a = 2.85)***	strong acid sites (pK_a = 9.4)****
1	SiO_2	3.7	0.5	11.9	1.9
2	OCP (0.5 h)/SiO_2	3.3	0.1	8.4	1.2
3	OCP (2 h)/SiO_2	2.5	0.02	6.7	1.1
4	OCP (6 h)/SiO_2	2.1	0.0	6.3	0.8
5	OCP (12 h)/SiO_2	1.9	0.0	2.2	0.0
6	Graphite [25]	1.5	0.0	2.6	0.0

* The initial concentration (C_0) of piperidine was 9.9 mmol/l.
** C_0 of diphenylamine was 3.9 mmol/l.
*** C_0 of *ortho*-bromobenzoic acid was 2.5 mmol/l.
**** C_0 of *para*-chlorophenol was 4.4 mmol/l.

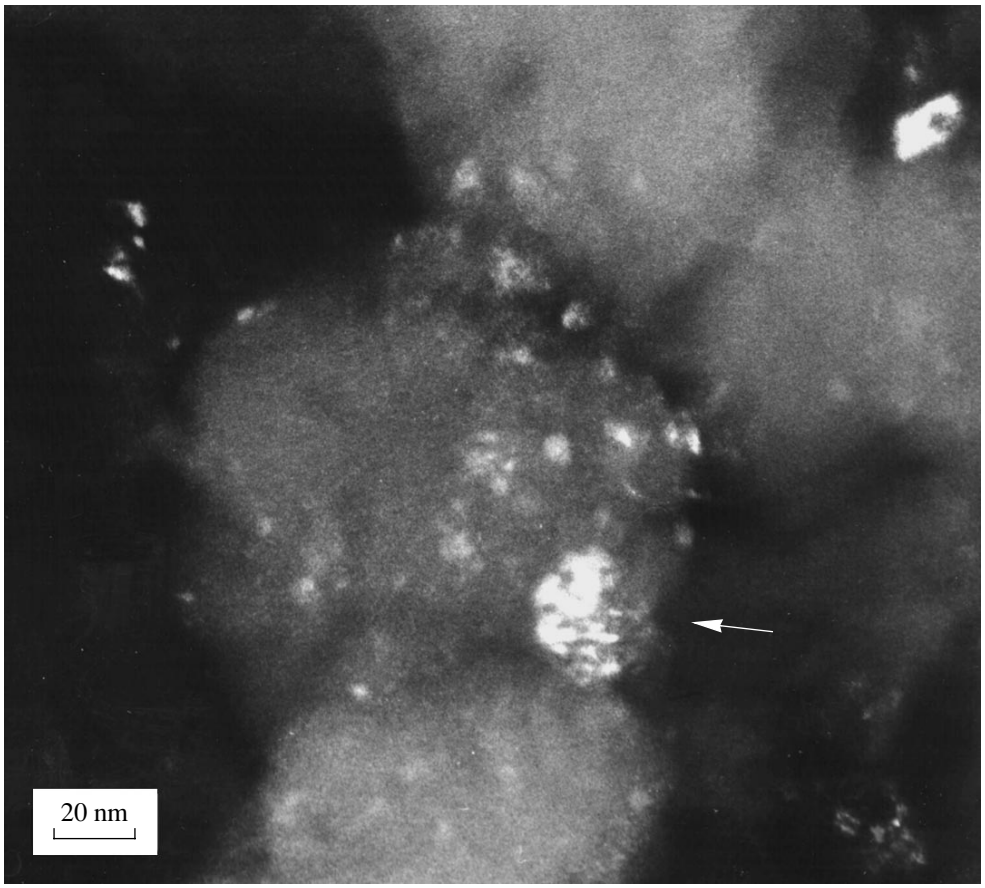

Fig. 4. Micrograph of sample OCP (12 h)/SiO_2 in a dark field. An arrow indicates deposited sulfur.

(Fig. 1b). C_2H_4, CH_4, CO_2, H_2O, H_2S, and sulfur, as well as C_2H_6, CO, COS, CS_2, and OCP in minor amounts, were formed along with propylene in the oxidative dehydrogenation of C_3H_8 by sulfur dioxide. The selectivity to cracking products (C_2H_4, CH_4, and C_2H_6) increased for 0.5 h and then gradually decreased. The selectivity to CO_2 decreased from 22 to 13% in 0.5 h. The formation of COS and CS_2 ceased completely within 6 h. A balance on carbon, calculated from gaseous products, increased from 79 to 98% in 0.5 h of operation.

The catalytic properties were changed simultaneously with changes in the state of the catalyst. We found that the deposition of OCP in the oxidative dehydrogenation reaction of propane at the stage of activation was accompanied by a change in the surface acid–base properties of silica (Table 1). According to IR-spectroscopic data obtained using low-temperature CO adsorption in accordance with the published procedure [19], SiO_2 (calcined at 640°C) used in this study exhibited weak acid sites (Si–OH groups) and stronger acid sites (Brønsted acid sites (BAS)) due to an Al impurity in the sample [20]. It is likely that the presence of basic sites is due to a sodium impurity. Table 1 indicates that, at the initial stage of formation of a carbon coating, a relatively sharp decrease in the concentrations of basic sites and, especially, strong acid sites was observed. According to published data [21–23], the BAS of aluminosilicates and zeolites are active in the formation of aromatic and polyphenyl condensation products from propane and propylene at high temperatures. An increase in the balance on carbon (Fig. 1b) suggests that a decrease in the rate of OCP deposition at the initial period of the reaction resulted from a dramatic decrease in the concentration of strong acid sites, which was observed over 0.5–2 h of catalyst operation. Loskutov and Khlopotov [24] reported that in the reaction of sulfur vapor with carbon materials a sodium impurity catalyzes the reaction of CS_2 formation. It is likely that a decrease in the selectivity to CS_2 and COS within ~6 h resulted from the simultaneous coverage of strong basic sites with OCP. The carbonization of the catalyst for 6–12 h of reaction, probably, causes the complete blocking of acid and basic sites of the initial SiO_2 and the formation of new sites, which are similar to graphite sites in properties [25]. Further coke accumulation (up to ~30–40 wt % C/SiO_2) was not accompanied by a dramatic change in the catalytic activity.

The formation of active OCP on SiO_2 was studied by DRIFT spectroscopy. At the initial stage of coke for-

mation, the DRIFT spectrum of sample OCP (0.5 h)/SiO_2 (OCP formed on the surface of SiO_2 in the course of reaction for 0.5 h) exhibited the appearance of absorption bands due to weakly condensed aromatic (probably, polyphenyl) compounds ($\nu_{C=C}$ 1503, 1580, and 1607 cm^{-1}; $\nu_{=C-H}$ 3010–3070 cm^{-1}) that have branched alkyl groups ($\nu_{C-H}(CH_3)$ 2870, 2950, and 2970 cm^{-1}; $\nu_{C-H}(CH_2)$ 2845 and 2920 cm^{-1}; $\delta(CH_3, CH_2)$ 1428, 1448, 1462, and 1380 cm^{-1} [26]) (Fig. 2a, spectrum *1*). The DRIFT spectrum of OCP formed in the course of reaction for 2–6 h exhibited absorption bands that are typical of condensed polycyclic aromatic structures with a low concentration of alkyl groups. Figure 2a demonstrates a change in the region of absorption bands due to benzene rings (1615 and 3010–3070 cm^{-1}) and alkyl groups (ν_{C-H} and $\delta_{HCH}(CH_3, CH_2)$), which can be indicative of an increase in the C/H ratio in OCP. The carbonization of a catalyst for 0.5–6 h in the course of reaction was accompanied by a successive decrease in the intensities of absorption bands due to the hydroxyl groups of the starting silica (ν_{O-H} 3740 and 3690 cm^{-1}) in the DRIFT spectrum and by the appearance of a broad absorption band at 3450 cm^{-1} due to hydroxyl groups perturbed by hydrogen bonds with the π systems of aromatic rings. Because the spectrum of a sample that operated for 12 h in the course of reaction did not exhibit absorption bands due to hydroxyl groups, it is believed that the surface of silica was completely covered with OCP during this period. The spectrum of OCP (12 h)/SiO_2 (Fig. 2b) exhibited absorption bands that are characteristic of the polyaromatic rings of highly condensed coke (the most intense absorption band is at $\nu_{C=C}$ 1580 cm^{-1}) [22, 27]. The spectra of studied OCP (0.5–12 h)/SiO_2 also exhibited absorption bands due to carbonyl ($\nu_{C=O}$ 1640 and 1695 cm^{-1}), carbonate–carboxylate (ν(RCOO) 1347, 1360, 1535, and 1555 cm^{-1}) and lactone groups ($\nu_{C=O}$(–C(O)OC) 1835 and 1860 cm^{-1}), which are typical of cokes and coals [27, 28]. Note that, according to DTA data, all of the OCP/SiO_2 samples exhibited no endothermic peak with a loss of weight at 100–130°C, which corresponds to the removal of adsorbed water.

The UV–VIS spectrum of OCP (0.5 h)/SiO_2 exhibited an intense absorption band at 260–265 nm, which was ascribed to the $\pi \longrightarrow \pi^*$ transition in monocyclic aromatic compounds, and a weak structureless absorption in the visible region, which is characteristic of graphite-like coke. The accumulation of a graphitized portion of OCP manifested itself in the spectra as a successive and strong increase in the background absorption in the visible region for samples operated for 0.5, 2, 6, and 12 h. According to Poluboyarov *et al.* [29], the optical absorption of coals and cokes in the visible region is due to their incompletely graphitized portion. The UV–VIS spectra of samples of OCP (2–12 h)/SiO_2 exhibited absorption bands at 240–250, 280–295, 320, 450–480, 560, 650–680, and 770 nm, whose intensities considerably increased with the time of exposure to the reaction mixture. On the one hand, absorption in this region can be due to the presence of polyconjugated aromatic structures (coke precursors) on the surface of silica: an absorption band at 280–295 nm and a shoulder at 320 nm can characterize the absorption of bicyclic aromatic compounds, and absorption at 300–800 nm can be due to aromatic structures with the number of conjugated rings as high as 12–19 for linear or 7–11 for nonlinear systems [21, 29, 30]. On the other hand, these absorption bands can be attributed to the absorption of sulfur compounds: sulfur polymers, 295 (S_2), 320 (S_8), and 450–480 nm (S_3 and S_4); sulfides (S^{2-}), a shoulder at 240–250 nm [31]; and C=S structures, absorption bands at 560 nm (the $\pi \longrightarrow \pi^*$ transition in thiobenzophenone analogues) [30]. The formation of C=S, C–S–C, and sulfur bridges between the layers of condensed carbon was mentioned in a number of publications on the treatment of various coal modifications with sulfur-containing compounds (SO_2, CS_2, H_2S, and sulfur vapor) [24]. Moreover, according to Poluboyarov *et al.* [29], free radicals of pyrolyzed organic compounds, which exhibit EPR spectra, can absorb radiation in the visible region. In accordance with these data, an absorption band at 770 nm in the UV–VIS spectrum can correspond to the $\pi \longrightarrow \pi^*$ transition in a polyconjugated organic radical with an odd number of carbon atoms and the number of hexagonal rings equal to five, whereas an absorption band at 450–480 nm can correspond to a radical with the number of rings equal to three.

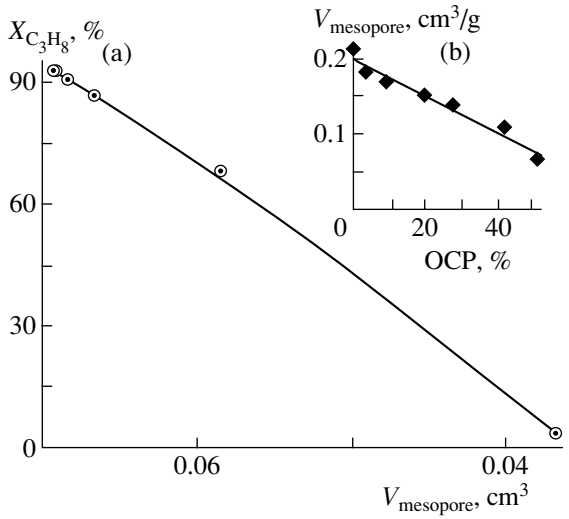

Fig. 5. Deactivation of OCP/SiO_2 in the course of the oxidative dehydrogenation of C_3H_8: (a) propane conversion ($X_{C_3H_8}$) as a function of the total mesopore volume of the catalyst; (b) a decrease in the mesopore volume on the accumulation of OCP in the course of reaction.

An electron-microscopic study demonstrated that OCP (6 h)/SiO_2 consisted of graphite-like strongly disordered coke. Coke deposits were formed by a heterogeneous mixture of particles, a portion of which was constituted of packets of several graphite planes. The basis layers in a packet were arranged irregularly; a three-dimensional order characteristic of graphite was not observed, and planes were swung through random angles about a normal to the plane of layers. The distance between graphite planes was d = 0.35 nm, which is greater than the interlayer spacing d = 0.3345 nm characteristic of graphite. The observed parameters are typical of coke with a turbostratic structure [32]. On the surface of SiO_2, coke was deposited as shells, twisted layered carbon nets, and it inhomogeneously covered the surface of support pellets (Fig. 3). An increase in the time of OCP deposition to 12 h resulted in a higher degree of coverage of the SiO_2 surface with coke. Carbon deposits form an inherent rough outer surface in contrast to the rounded surface typical of starting silica. Crystals of size 6–10 nm, whose morphology is characteristic of polymer sulfur, were detected on the surface of coked silica pellets and at pore openings (Fig. 4). The crystals of sulfur were arranged chaotically and nonuniformly over the sample surface.

According to chemical analysis data, the C : H atomic ratio in the active coke of samples OCP (6–12 h)/SiO_2 was approximately equal to 1 : (0.4–0.3). It is likely that OCP carbon networks consisted of a three-dimensional carbon polymer whose atoms are incorporated in graphitized and condensed aromatic structures cross-linked to each other by alkyl or sulfur bridges. The quinone, C=S, lactone, carboxyl, and alkyl groups, which were detected by diffuse-reflectance spectroscopy, are probably the terminal substituents of polynuclear structures.

Thus, at the initial stage of activation, coke precursors rapidly blocked the acid sites of initial silica. It is likely that in the further course of reaction both the growth and condensation of carbon networks formed at the acid sites and the formation of new networks because of homogeneous reactions took place. The coverage of the initial surface of silica pellets by a carbon material and the accumulation of an active OCP phase were accompanied by the attainment of a quasi-steady state in catalyst operation. To reveal the properties of active OCP, they were compared with deactivated samples.

Table 2. Changes in the texture characteristics of silica in the course of coking

Entry	Conditions of OCP formation			S_{sp}, m^2/g		V_{pore} (from saturation), cm^3/g	$V_{micropore}$, cm^3/g	D_{av}^{**}, nm	Pore volume distribution, cm^3/g		
	mixture*	T, °C	t, h	BET	t-method				D = 4–10 nm	D = 10–100 nm	D = 100–1000 nm
1	Initial***			40	–	0.222	0.000	24.2	0.012	0.138	0.072
2	I	640	0.5	39.8	–	0.212	0.000	21.2	0.012	0.137	0.063
3	I	640	2	39.4	–	0.182	0.000	19.4	0.012	0.139	0.031
4	I	640	5	39.4	41.1	0.170	0.001	14.9	0.013	0.127	0.029
5	I	640	12	39.4	39.8	0.156	0.004	14.9	0.013	0.111	0.019
6	I	640	30	118.6	38.7	0.172	0.033	7.0	0.030	0.100	0.019
7	I	640	60	122.9	36.2	0.155	0.045	5.1	0.031	0.061	0.018
8	I	640	105	165.4	31.5	0.133	0.068	3.2	0.033	0.014	0.018
9	II	640	4	31.5	31.5	0.135	0.000	17.1	0.012	0.100	0.023
10	II	800	3	20.9	21.9	0.114	0.001	21.8	0.009	0.087	0.015
11	II	800(850)	7(6)	5.5	7.6	0.035	0.002	25.2	0.013	0.020	0.001

*** I**, $C_3H_8 : SO_2 : He : N_2 = 10 : 10 : 79 : 1$ vol %; **II**, $C_3H_8 : SO_2 : N_2 = 79.5 : 19.5 : 1$ vol %. The temperature and time of additional treatment are given in parentheses.

** The average pore diameter was calculated by the equation $D_{av} = 4V/S_{BET}$.

*** SiO_2 without contact with a mixture.

A Study of Deactivated Catalysts

The deposition of OCP in the course of reaction changed the texture of the catalyst. The starting silica exhibited a mesoporous structure with a predominant pore diameter of $D \sim 30$–50 nm (Table 2, entry 1). Carbonization in the course of reaction was accompanied by a gradual decrease in the volume and average diameter of pores (Table 2, entries 2–8). Figure 5b shows that the volume of mesopores linearly decreased with the deposition of OCP. The coke density can be estimated by the equation $\rho_C = K/(V_0(1 - K) - V_K)$ [32], where K is the coke content of the sample (g/g), and V_0 and V_K are the pore volumes of the initial and carbonized samples, respectively. The average density of carbon deposits is $\rho_C \approx 1.5$ g/cm^3; this value indicates that coke was deposited in the volume of mesopores without blocking pore openings [32]. At the initial stage of coke deposition, the volume of coarse transport pores, which are connected to the surface by the widest openings (D = 100–1000 nm), decreased (Table 2, entries 2, 3); that is, coke was deposited on the surface of secondary aggregates. After the blocking of active centers, the process of coking was transferred to cavities with the widest openings in the bulk of aggregates: the accumulation of more than 9 wt % OCP resulted in a gradual decrease in the volume of mesopores with a diameter of 10–100 nm, an increase in the volume of pores with narrower openings (D = 4–10 nm), and the formation of micropores 1.0–1.1 nm in diameter (Table 2, entries 4–8). The specific surface areas S_{sp}(BET) of samples increased upon the deposition of OCP; however, these values may be overestimated because of the formation of micropores in the coke structure (Table 2, entries 6–8). The values of S_{sp} calculated by the *t*-method [14] insignificantly decreased in the course of coking.

Previously [13], it was found that the texture of catalysts (aluminosilicates) significantly affected the oxidative dehydrogenation reaction of C_3H_8 in the presence of SO_2: the rate of propane conversion at a reaction temperature of 640–700°C was proportional to the volume of mesopores. Figure 5a indicates that carbon deposition in SiO_2 mesopores in the course of reaction decreased the conversion of propane ($X_{C_3H_8}$). At < 40 wt % of accumulated coke, the conversion of propane decreased by ~30% and selectivity to propylene increased, whereas the conversion of propane dramatically decreased to 3.4%, the yield of propylene decreased to 1%, and the fraction of CO_2 in the reaction products increased at >40 wt % of deposited OCP (Fig. 1b). It is likely that a considerable decrease in the average pore diameter to 3–5 nm in the course of considerable coke deposition imposed diffusion limitations on both propane conversion and selectivity to the products of propane conversion.

The special features of OCP formed in the course of reaction can be determined by a comparative study of active and deactivated samples. We found using DTA that, as the amount of OCP deposited on SiO_2 increased from 3.5 to ~20 wt %, the maximum exothermic effect

Table 3. Deposition of OCP on SiO_2 in the course of the oxidative dehydrogenation of propane according to thermal analysis data

Entry	Sample	OCP content, wt %	T_{max} of the exothermic effect of coke burning, °C (Δm, wt %)		
1	OCP (2 h)/SiO_2 (**I**)*	3.5	550	–	–
2	OCP (6 h)/SiO_2 (**I**)	9	550	–	–
3	OCP (12 h)/SiO_2 (**I**)	20	560	–	–
4	OCP (30 h)/SiO_2 (**I**)	28	565 (26)	680 (~2)	–
5	OCP (60 h)/SiO_2 (**I**)	42	565 (38)	680 (4)	–
6	OCP (105 h)/SiO_2 (**I**)	51	570 (40)	680 (11)	–
7	OCP (4 h)/SiO_2 (**II**)**	37	565	–	–
8	OCP (3 h)/SiO_2 (**II**/a)***	44	570 (18)	635 (~4)	725 (22)
9	OCP (7 h)/SiO_2 (**II**/a)	50.5	570 (8)	640 (13)	720 (29.5)
10	OCP (15 h)/SiO_2 (**II**/a)	59.5	–	–	720
11	Carbon (Sibunit)	98.3	–	–	715

* Treated with mixture **I**; T [OCP formation] = 640°C.

** Treated with mixture **II**; T = 640°C.

*** Treated with mixture **II**; T = 800–850°C.

of their elimination (T_{max}) remained almost unchanged and equal to 550–560°C (Table 3, entries 1–3). Consequently, the degree of condensation of coke deposits did not increase in this case [23, 33]. According to the electron-microscopic data considered above, coke of this type was deposited as shells and scales on the surface. The accumulation of more than 28% OCP (in catalyst operation for longer than 30 h) was accompanied by a further increase in the degree of coke condensation with an increase in the value of T_{max} from 550 to 570°C (Table 3, entries 4–6) and by the appearance of more highly condensed compounds, which are characterized by T_{max} = 680°C. It is likely that the formation of these highly condensed OCP was accompanied by a slow process of burning of the layers of a less condensed coke portion under oxidative reaction conditions to result in the appearance of slitlike micropores (Table 2, entries 6–8). This fact was supported by the formation of only one type of OCP with T_{max} = 565°C on the rapid carbonization of the catalyst (37% OCP in the oxidative dehydrogenation of concentrated mixture **II** for 4 h, as compared with 42% OCP in mixture **I** for 60 h of operation (Table 3, entries 5 and 7)). The formation of micropores was not observed on rapid coke deposition (Table 2, entry 9).

To study the effect of the degree of condensation of OCP on their catalytic activity, we performed a series of high-temperature (750–850°C) treatments of the catalyst with concentrated mixture **II**. These treatments were favorable for the burning of low-temperature coke. According to DTA data, OCP with T_{max} = 570 and 635°C (Table 3, entry 8) and carbon-like deposits with a maximum of the exothermic effect of burning close to that of Sibunit (Table 3, entry 11) were formed on the surface of a sample calcined at 800°C for 3 h. An increase in the time of high-temperature treatment at 800°C up to 7 h resulted in the burning of OCP with T_{max} = 570°C and in the accumulation of highly condensed OCP and carbon-like deposits. Sample OCP (15 h)/SiO_2(II/a) (a denotes a sample calcined in reaction mixture **II** at 800–850°C) did not bear OCP on its surface; it contained only carbon-like deposits (Table 3, entry 10).

Table 4 summarizes the effects of coke formation conditions on catalytic activity. It can be seen that OCP formed on the treatment of the catalyst with mixture **II** at 750–800°C exhibited an activity similar to the activity of OCP formed in the course of reaction at 640°C (Table 4, entries 1–6). However, an increase in the time of high-temperature treatments considerably decreased

Table 4. Effect of the conditions of OCP formation on the surface of SiO_2 in the course of the oxidative dehydrogenation of propane on the catalytic properties (mixture **II**; $\tau_{contact}$ = 10 s, T = 640°C)

Entry	Conditions of OCP formation*		$x_{C_3H_8}$, %	Selectivity, %			
	T, °C	t, h		C_3H_6	C_2H_4	CH_4	CO_2
1	640	4	70.7	45.7	12.4	18.4	11.8
2	750	1	69.8	43.3	13.8	20.4	8.9
3	800	1	71	41	15.2	22.5	4.9
4	″	3	71.3	39.4	16.5	23.7	4.2
5	″	5	68.4	36	20.6	26.9	2
6	″	7	69	31	21.8	28.8	1.2
7	800 (850)	7 (2)	39.1	26.1	26	36	0
8	″	7 (6)	14.2	0	40.5	49.5	0

* The temperature and time of an additional treatment are given in parentheses.

Table 5. Binding energies and atomic ratios between elements on the surface of OCP/SiO_2 catalysts

Entry	Sample*	E_b, eV			Atomic ratios between elements			
		C1*s*	S2*p*	O1*s*	C/Si	S/Si	O/Si	S/C
1	OCP (2 h)/SiO_2 (**I**)	284.6	*	532.3	0.45	–	2.7	–
2	OCP (6 h)/SiO_2 (**I**)	284.5	162.7	532.3	1.47	0.052	2.7	0.035
3	OCP (105 h)/SiO_2 (**I**)	284.6	164.5	532.4	6.67	0.57	2.9	0.085
4	OCP (4 h)/SiO_2 (**II**)	284.7	164.4	532.4	6.85	0.3	2.9	0.045
5	OCP (3 h)/SiO_2 (**II**/a)	284.7	164.2	532.4	5.15	0.122	2.8	0.026
6	OCP (15 h)/SiO_2 (**II**/a)	284.5	164.3	532.4	11.23	0.232	3.6	0.023

* Below the detection limit of the method (S/Si < 0.005).

selectivity to propylene and resulted in an increase in selectivity to cracking products. An additional treatment of the catalyst with reaction mixture **II** at 850°C for 2 h decreased $X_{C_3H_8}$ from ~70 to 39.1%; additional heating for 4 h resulted in a further decrease in propane conversion; in this case, selectivity to propylene decreased to 0% (Table 4, entries 7, 8). A study of the texture of these samples demonstrated that the treatment of the catalyst with a concentrated mixture at a high temperature resulted in losses in the specific surface areas and pore volumes. However, the average pore diameter did not decrease upon this treatment; micropores were not formed, and the volume of pores 4–10 nm in diameter did not increase (Table 2, entries 9–11). Consequently, a decrease in the reaction selectivity with increasing time of high-temperature treatments was due to the formation of more condensed coke with T_{max} 635–640°C rather than to diffusion limitations.

The data allowed us to conclude that low-temperature OCP with a maximum of the exothermic effect of burning at 550–570°C are most selective in the formation of propylene. The formation of more highly condensed OCP with T_{max} 635–680°C resulted in a decrease in the selectivity; carbon-like deposits are inactive in the formation of propylene. A sequential decrease in selectivity to deep oxidation products to 0% in the course of high-temperature treatments (Table 4) suggests that CO_2 is formed in the oxidation of low-temperature OCP $SO_2 + C \longrightarrow CO_2 + S$. A similar assumption was made by Lisovskii and Alkhazov [4, 34], who studied the oxidative dehydrogenation of ethylbenzene on OCP/Al_2O_3.

An XPS Study of OCP/SiO$_2$

The survey spectra of the test samples exhibit the photoelectron and Auger lines of silicon, oxygen, carbon, and sulfur. Table 5 summarizes data on the binding energies and the atomic ratios between elements on the surface. In all OCP/SiO_2 samples, the C1*s* binding energies were found to be equal to 284.5–284.7 eV; this value is close to the tabulated data for graphite (284.3–284.6 eV [15]). The C1*s* binding energies of active and deactivated samples were almost equal; therefore, it was impossible to monitor the formation of graphite-like structures, which are responsible for catalyst deactivation. The ratio C/Si at the surface increased as the duration of catalyst operation increased from 2 to 105 h (Table 5, entries 1–3). The ratio C/Si in sample OCP (2 h)/SiO_2(I) (treated with reaction mixture **I**) was 0.45; consequently, most of the surface was not covered by OCP. An increase in the time of exposure to the reaction mixture up to 6 h (Table 5, entry 2) resulted in almost complete surface coverage with carbon-like deposits; this was accompanied by an increase in the selectivity $S_{C_3H_6}$ from 35 to 43% (Fig. 1b). The oxidative dehydrogenation of concentrated mixture **II** resulted in the accelerated accumulation of coke deposits on the surface of silica (Table 5, entries 1, 2, and 4). The surface carbon concentrations in activated OCP (4 h)/SiO_2(II) (treated with reaction mixture **II**) and deactivated sample OCP (105 h)/SiO_2(I) were similar (C/Si = 6.85 and 6.67, respectively). Consequently, catalyst deactivation depended on the nature rather than the amount of carbon deposited on the surface, as discussed above. The O1*s* binding energies in all of the samples were found to be 532.3–532.4 eV; these values are close to the tabulated data for oxygen in the SiO_2 molecule (532.7 eV [15]). It is likely that the superstoichiometric ratio O/Si in the range 2.7–2.9 resulted from the presence of oxygen-containing compounds at the surface of OCP/SiO_2 (quinone, lactone, and carboxylate structures, which were detected by IR spectroscopy). In sample OCP (15 h)/SiO_2(II/a), oxygen localized in the interplanar faces of graphite can additionally contribute to the O1*s* signal (O/Si = 3.6). In the majority of the test samples, the S2*p* binding energies were calculated to be 164.2–164.5 eV, which corresponds to the S^0 state of surface sulfur [15]. Sulfur is the product of SO_2 conversion, and it is accumulated on the surface of OCP in the course of reaction (Table 5, entries 1–3). A considerable decrease in SO_2 conversion for deactivated sample OCP (105 h)/SiO_2(I) and, hence, a decrease in the yield of elemental sulfur would result in the rapid removal of sulfur molecules from the surface because the reaction temperature (640°C) was much higher than the boiling temperature of sulfur (444.6°C). However, both total and relative sulfur contents (S/Si and S/C) of this sample were maximal (Table 5, entry 3); this fact can be explained by the incorporation of elemental sulfur into the structure of OCP. This conclusion was supported by a considerable sulfur content (S/C) of OCP in samples subjected to high-temperature treatment (Table 5, entries 5, 6). In sample OCP (6 h)/SiO_2(**I**), which was selective in propylene formation, the S2*p* binding energy was calculated to be 162.7 eV, which corresponds to the S^{2-} state of surface sulfur [15]. The presence of a large amount of elemental sulfur on the surfaces of other active samples (Table 5, entries 4, 5) did not allow us to observe signals due to S^{2-}.

Osipova and coauthors [10, 11] found that the yield of propylene in the oxidative dehydrogenation of propane increased as the sulfur content (in the state S^0) of OCP increased. According to our data, deactivated samples OCP (105 h)/SiO_2(I) and OCP (15 h)/SiO_2(II/a) contained considerable amounts of elemental sulfur: the S/C ratios were equal to 0.085 and 0.023, respectively (Table 5, entries 3 and 6). A study of sample OCP (6 h)/SiO_2(I), which was active and selective in propylene formation, demonstrated that the concentration of sulfur in the state S^0 in OCP was insignificant, and it was not detected using this technique. Thus, it is impossible to correlate the elemental sulfur content of a sample with the catalytic activity.

An EPR Study of OCP/SiO_2

It was found [4, 7, 9] that the yield of styrene in the oxidative dehydrogenation of ethylbenzene increased symbatically with an increase in the concentration of unpaired electrons in OCP formed on the surface of alumina in the course of reaction. It was assumed that the paramagnetic centers of coke are the active centers of this reaction. In this context, it was of interest to examine OCP formed in the reaction of oxidative propane dehydrogenation on the surface of SiO_2.

The EPR spectra of active and deactivated samples OCP/SiO_2 are characterized by a line with the *g*-factor close to the *g*-factor of free electron (g_e = 2.0023), which was observed in various cokes and coals. This *g*-factor is characteristic of polyconjugated aromatic radicals [29]; a shift of the *g*-factor toward greater values (up to 2.004) was observed when oxygen or sulfur entered the radical structure with a considerable spin–orbital coupling constant. An EPR signal with the *g*-factor 2.0031, which was ascribed to an oxygen-containing radical with an anthraquinone structure, was observed in a study of coked Al_2O_3 in the oxidative dehydrogenation of ethylbenzene to styrene at 450°C [7]. However, according to Vasil'eva [35], these radicals do not exist at the elevated temperature (640°C) at which the oxidative dehydrogenation of propane takes place.

The initial silica did not exhibit signals in the EPR spectrum. Table 6 summarizes the characteristics of EPR signals of coked silicas. The true intensity of the EPR signals of the test samples cannot be determined because of their high conductivity. The conductivity of samples increased with the amount of OCP. To obtain information on the nature of electronic paramagnetism in carbonized samples, the following properties of the paramagnetic centers of coals and cokes can be used: the sensitivity to oxygen adsorption and to the degree of condensation, the temperature dependence of the signal width, and the shape of the EPR line [29, 35–38]. On the addition of oxygen to evacuated samples of condensed coke systems, the oxygen effect—the broadening of EPR spectra because of the interaction of the paramagnetic molecules of adsorbed oxygen (s = 1) with the paramagnetic centers of a carbon structure—can be observed [36]. The temperature dependence of the line width and the oxygen effect can be explained taking into account energy exchange between the detected paramagnetic centers (C) and a paramagnetic impurity (P), such as adsorbed oxygen, through conduction electrons (S) in terms of the models of *C–S-*, *C–S–L-* (L is a lattice), or *C–S–P* relaxation [29, 37]. Highly condensed cokes can exhibit spectra with a Dyson line shape or a distorted Dyson line shape, which is associated with the appearance of small conducting areas and conduction electrons [38]. In actual practice, the Dyson distortion of an EPR line is observed when the ratio between the times T_D (the time of conduction-electron diffusion through a skin layer) and T_L (the time of conduction-electron diffusion through the entire sample or the conducting area) in comparison with T_{SL} (spin–lattice relaxation time) and T_2 (spin–spin relaxation time) should be taken into account. A detectable distortion of the spectrum toward a Dyson shape is observed on conditions that $T_L \gg T_D$ and $T_L \gg T_{SL}$. At $T_L \gg T_2 > T_D$ and $T_L \gg T_D > T_2$, symmetric and asymmetric distortions, respectively, are observed. Otherwise, there is no Dyson distortion of an EPR line, and a Lorentzian or Gaussian line is observed.

In a study of the EPR spectra of paramagnetic centers in samples OCP (6 h)/SiO_2(I), OCP (4 h)/SiO_2(II), and OCP (3 h)/SiO_2(II/a), which were active and selective in the formation of propylene, the following two phenomena were found (Table 6, entries 1, 3, and 4):

(1) The observed temperature dependence of the line width of an EPR signal and the broadening of the spectra on the addition of oxygen are a consequence of the interaction of the unpaired localized electrons of carbon atoms with an electron gas (a gas of delocalized

Table 6. Characteristics of the EPR signals of carbonized samples

Entry	Sample	ΔH_{vacuum}, G		EPR line shape (conditions of observation)	ΔH_{air}, G	
		77 K	300 K		77 K	300 K
1	OCP (6 h)/SiO_2 (**I**)	18.4	31.9	Slightly asymmetric, Dyson distortion: $T_D > T_2$ (77, 300 K)	*	*
2	OCP (105 h)/SiO_2 (**I**)	10.4	32.5	Symmetric (vacuum, 77 K); symmetric, Dyson distortion: $T_D/T_2 \longrightarrow 0$ (vacuum, 300 K; air, 77, 300 K)	15.7	110**
3	OCP (4 h)/SiO_2 (**II**)	5.2	8	Asymmetric, Dyson distortion (77, 300 K)	13.5, 52	78.4
4	OCP (3 h)/SiO_2 (**II**/a)	24.5	29	Slightly asymmetric, Dyson distortion: $T_D > T_2$ (vacuum, 77, 300 K); asymmetric Dyson line: $T_D/T_2 \longrightarrow \infty$ (air, 77, 300 K)	55.1	59.6
5	OCP (15 h)/SiO_2 (**II**/a)	1.2	2.08	Symmetric, high conductivity without Dyson distortion	***	***

* Considerable broadening (ΔH > 350 G) makes the observation of EPR spectra difficult to perform.

** ΔH = 46 G (300 K; air, 1 torr).

*** The EPR signal is insensitive to oxygen.

electrons), which characterizes the disordered region of graphite networks.

(2) It is likely that the observed distortion of the EPR line shape of the Dyson type is due to the interaction of localized electrons with an electron gas by distorting a microwave field, and it is associated with the anomalously high conductivity of a gas of delocalized electrons in the regions of OCP paramagnetic centers, which is comparable to the conductivity of an electron gas in metals. This phenomenon is indicative of the appearance of the long-range ordering of highly ordered graphite-like networks. The detection of a pure Dyson line in sample OCP (3 h)/SiO_2(II/a) is indicative of the appearance of large high-conductivity regions of a graphite-like phase.

In deactivated sample OCP (105 h)/SiO_2(I), the temperature dependence of the line width, the oxygen effect, and the Dyson distortion of the line shape were observed, which are typical of active samples (Table 6, entry 2). The sample exhibited a much higher conductivity than that of OCP (6 h)/SiO_2(I); this can be explained by the greater weight of the coke formed (51 and 9%, respectively (Table 3, entries 2 and 6)). It is likely that the low yield of propylene on this sample (at 35% selectivity) is due to a decrease in the conversion of propane because of diffusion limitations caused by a decrease in the pore size on coking.

The absence of the oxygen effect and the Dyson distortion of the line shape in the presence of the temperature dependence of the line width (at a very high conductivity) for sample OCP (15 h)/SiO_2(II/a) (Table 6, entry 5), which was nonselective in propylene formation, is indicative of, on the one hand, the existence of regions where paramagnetic centers and conduction electrons occur and, on the other hand, the existence of large "reservoirs" of conduction electrons, which make it possible to completely eliminate the effect of adsorbed oxygen. This indicates that the high-conductivity sites and the sites of localized unpaired electrons are separated in the bulk of coke deposits, and they interact with each other only slightly. It is of paramount importance that, in addition to conducting graphite-like deposits, which do not exhibit an EPR spectrum, the formation of loose coke with a high degree of condensation, which gives a narrow EPR signal at 1.2 G, was observed. The presence of highly condensed coal-like coke was also detected using DTA by the appearance of a peak with a maximum burning temperature of 725°C (Table 3, entry 10).

We can assume that the paramagnetic centers of OCP, which are observed by EPR spectroscopy, can participate in the dissociation of the oxidant molecule to form active oxygen and sulfur species, which react with propane molecules with the formation of alkyl radicals.

CONCLUSIONS

Oxidative condensation products on the surface of silica, which are active and selective in the oxidative dehydrogenation of propane to propylene in the presence of SO_2, are disordered carbon layered networks chaotically arranged on the SiO_2 surface. They include a graphitized portion and condensed polyaromatic structures, which are linked together by alkyl or sulfur bridges. Quinone, lactone, carboxyl, and alkyl terminal substituents were detected in the structure of these networks.

Structural changes in OCP were detected in the course of their accumulation. Less condensed OCP with a maximum exothermic effect of burning at 550–570°C were initially formed. Sulfur in the state S^0 was deposited at the surface of these OCP; sulfur in the state S^{2-} was a constituent of these structures. In the course of reaction, a less condensed portion of OCP was slowly burned to form micropores, and highly condensed OCP with a maximum exothermic effect of burning at 635–680°C were formed. We found that sulfur in the state S^0 was encapsulated in the structure of these OCP. The accumulation of such OCP decreased selectivity to propylene.

Catalyst deactivation may be due to considerable coke deposition, which results in a decrease in the volume and radius of pores; this coke deposition imposed diffusion limitations on both the conversion of propane and the selectivity to the conversion products.

We found that carbon-like deposits (with a maximum exothermic effect of burning at 725°C) formed by the high-temperature degradation of active OCP are inactive in the formation of propylene.

ACKNOWLEDGMENTS

We are grateful to E.V. Kuznetsova for the determination of the acid–base properties of carbonized silicas.

REFERENCES

1. Iwasawa, Y., Nobe, H., and Ogasawara, S., *J. Catal.*, 1973, vol. 31, no. 3, p. 444.
2. Manassen, J. and Knalif, S.H., *J. Catal.*, 1969, vol. 13, no. 3, p. 290.
3. Gallard-Nechtschein, J., Pecher-reboul, A., and Traynard, Ph., *J. Catal.*, 1969, vol. 13, no. 2, p. 261.
4. Lisovskii, A.E., *Doctoral (Chem.) Dissertation*, Moscow: Inst. of Chemical Physics, 1983.
5. Alkhazov, T.G. and Lisovskii, A.E., *Okislitel'noe degidrirovanie uglevodorodov* (Oxidative Dehydrogenation of Hydrocarbons), Moscow: Khimiya, 1980, p. 240.
6. Echigova, E., Sano, H., and Tanaka, M., *Proc. 8th Int. Congr. on Catalysis*, Amsterdam: Elsevier, 1984, vol. 5, p. 623.
7. Cadus, L.E., Gorriz, O.F., and Rivarola, J.B., *Ind. Eng. Chem. Res.*, 1990, vol. 29, p. 1143.
8. Niva, M., Sago, M., and Murakami, Y., *J. Catal.*, 1981, vol. 69, no. 1, p. 69.

9. Fiedorow, R., Przystajko, W., Sopa, M., and Dalla Lana, J.G., *J. Catal.*, 1981, vol. 68, no. 1, p. 33.
10. Osipova, Z.G., Ushkov, S.V., Sokolovskii, V.D., and Kalinkin, A.V., *New Developments in Selective Oxidation*, Genti, G. and Trifiro, F., Eds., Amsterdam: Elsevier, 1990, p. 527.
11. Ushkov, S.V., Osipova, Z.G., and Sokolovskii, V.D., *React. Kinet. Catal. Lett.*, 1988, vol. 36, no. 1, p. 97.
12. Ushkov, S.B., Osipova, Z.G., Sokolovskii, V.D., and Ketchik, S.V., *Kinet. Katal.*, 1988, vol. 29, no. 1, p. 222.
13. Danilova, I.G. and Ivanova, A.S., *Kinet. Katal.*, 2000, vol. 41, no. 4, p. 622.
14. Gregg, S. and Sing, K., *Adsorption, Surface Area, and Porosity*, New York: Academic, 1982.
15. Nefedov, V.I., *Rentgenoelektronnaya spektroskopiya khimicheskikh soedinenii: Spravochnik* (X-ray Electron Spectroscopy: A Handbook), Moscow: Khimiya, 1984.
16. *Practical Surface Analysis by Auger and X-ray Photoelectron Spectroscopy*, Briggs, D. and Seah, M., Eds., New York: Wiley, 1983, p. 220.
17. Kovalenko, G.A. and Vanina, M.P., *Zavod. Lab.*, 1999, vol. 65, no. 9, p. 43.
18. Boehm, H.-P. and Knosinger, H., *Catalysis – Science and Technology*, Anderson, J.R., Ed., Moscow: Springer, 1984, vol. 4, p. 39.
19. Paukshtis, E.A., *Infrakrasnaya spektroskopiya v geterogennom kislotno-osnovnom katalize* (Infrared Spectroscopy in Heterogeneous Acid–Base Catalysis), Novosibirsk: Nauka, 1992, p. 256.
20. Panchenko, V.N., Semikolenova, N.V., Danilova, I.G., *et al.*, *J. Mol. Catal.*, 1999, vol. 142, no. 1, p. 27.
21. Kustov, L.M., Zholobenko, V.L., and Kazanskii, V.B., *Kinet. Katal.*, 1988, vol. 29, no. 4, p. 928.
22. Eisenbach, D. and Gallei, E., *J. Catal.*, 1979, vol. 56, no. 3, p. 377.
23. Yakerson, V.I., Nissenbaum, V.D., Vasina, T.V., *et al.*, *Izv. Akad. Nauk SSSR, Ser. Khim.*, 1990, no. 6, p. 1244.
24. Loskutov, A.I. and Khlopotov, M.N., *Adsorbtsiya i adsorbenty* (Adsorption and Adsorbents, 1981, no. 9, p. 86.
25. Kovalenko, G.A., Kuznetsova, E.V., Mogilnykh, Yu.I., *et al.*, *Carbon*, 2001, vol. 39, p. 1033.
26. Nakanishi, K., *Infrared Absorption Spectroscopy*, Tokyo: Holden Day, 1962, p. 216.
27. Dandecar, A., Baker, R.T.K., and Vannice, M.A., *Carbon*, 1998, vol. 36, no. 12, p. 1821.
28. Meldrum, B.J. and Rochester, C.H., *J. Chem. Soc., Faraday Trans.*, 1990, vol. 86, no. 5, p. 861.
29. Poluboyarov, V.A., Andryushkova, O.V., Bulynnikova, M.Yu., *Izv. Sib. Otd. Ross. Akad. Nauk, Ser. Khim. Nauk*, 1992, vol. 5, p. 5.
30. Nurmukhametov, R.N., *Pogloshchenie i lyuminestsentsiya aromaticheskikh soedinenii* (Absorption and Luminescence of Aromatic Compounds), Moscow: Khimiya, 1971, p. 216.
31. Karge, H.G., Lanieski, M., and Ziotek, M., *J. Catal.*, 1988, vol. 109, no. 1, p. 252.
32. Fenelonov, V.B., *Poristyi uglerod* (Porous Carbon), Novosibirsk: Inst. of Catalysis, 1995, p. 518.
33. Buyanov, R.A., *Zakoksovyvanie katalizatorov* (Catalyst Coking), Novosibirsk: Nauka, 1983, p. 207.
34. Alkhazov, T.G. and Lisovskii, A.E., *Kinet. Katal.*, 1976, vol. 17, no. 2, p. 434.
35. Vasil'eva, L.M., *Cand. Sci. (Chem.) Dissertation*, Novosibirsk: Institute of Catalysis, 1973.
36. Blyumenfel'd, L.A., Voevodskii, V.V., and Seienov, A.G., *Primenenie elektronnogo paramagnitnogo rezonansa v khimii* (Application of Electron Paramagnetic Resonance in Chemistry), Novosibirsk: Nauka, 1962, p. 205.
37. Ravilov, R.T., *Cand. Sci. (Chem.) Dissertation*, Novosibirsk: Inst. of Catalysis, 1980.
38. Poole, Ch., *Electron Spin Resonance: A Comprehensive Treatise on Experimental Techniques*, New York, 1970, p. 120.